Available online at www.sciencedirect.com
ScienceDirect
International Journal of Heat and Fluid Flow 28 (2007) 483–495
International Journal of HEAT AND FLUID FLOW
www.elsevier.com/locate/ijhff

Natural convection around a horizontal solid cylinder wrapped with a layer of fibrous or porous material

M. Ait Saada [a], S. Chikh [a,*], A. Campo [b,*]

[a] Faculté de Génie Mécanique et Génie des Procédés, USTHB B.P. 32, El Alia, Bab Ezzouar 16111, Algeria
[b] Department of Mechanical Engineering, University of Vermont, Burlington, VT 05405, USA

Received 18 December 2005; received in revised form 9 May 2006; accepted 17 May 2006
Available online 23 October 2006

Abstract

Heat losses in duct flow and heat transfer enhancement are investigated through an analysis of natural convection about a horizontal cylinder with a porous or fibrous coating. The porous substrate may be used for two purposes. According to its properties, it may be employed as an insulating material or as a means to surface augmentation. An optimization study is then carried out in order to find the best conditions that allow good thermal insulation or heat transfer rate improvement. The flow motion and heat transfer coefficient are predicted for various conditions. The results show that an efficient insulation which means less than 10% in heat losses is obtained for a porous layer thickness of 0.8× tube diameter and a permeability corresponding to $Da \leqslant 10^{-7}$. Nevertheless, there is a Darcy number limit above which convection must be accounted for. Porous or fibrous materials may also be used as a heat transfer augmentation technique. To achieve this goal, porous media with high permeability and/or high effective thermal conductivity must be selected.

Keywords: Natural convection; Horizontal cylinder; Porous medium; Heat losses

1. Introduction

There has been a lot of interest in the field of convective heat transfer through a saturated porous medium due to broad range of applications. A better understanding of convection through porous media can be of valuable contribution in several areas like insulation design, grain storage, geothermal systems, heat exchangers, filtering devices, metals processing, catalytic reactor, etc. Thermal insulation of ducts subject to high temperature gradients as well as use of porous materials as a means to heat transfer enhancement in tubular heat exchangers are important problems related to convection through porous media. The thermal insulator typically consists of fibrous or porous material which is permeable to air. Consequently, natural convection may arise in the insulating material. Thus, accounting for thermal convection in the porous layer covering the cylinder may be very useful for the analysis of thermal insulation optimization or heat transfer enhancement.

Flow in infinite fluid medium is characterized by the boundary layer development around a horizontal isothermal circular cylinder ($10^4 \leqslant Ra \leqslant 10^8$). Kuehn and Goldstein (1980) considered the curvature effects and the pressure difference across the boundary layer and applied a numerical procedure based on finite differences to solve Navier–Stokes and energy equations in steady state conditions ($Pr = 0.7$ or 7). Their numerical and experimental results are in good agreement with those existing in the literature. Farouk and Guceri (1981) followed the same procedure to study the case of a cylinder with uniform temperature ($Pr = 0.721$ and $1 \leqslant Ra \leqslant 10^7$), while Qureshi and Ahmed (1987) analyzed the constant heat flux case ($Pr = 0.7$ and $10^2 \leqslant Ra \leqslant 10^7$). Later, Song (1989) studied numerically the transient natural convection around a horizontal electric wire with a uniform temperature

* Corresponding authors. Tel.: +1 802 656 0978; fax: +1 802 656 1929 (A. Campo).
E-mail addresses: salahchikh@yahoo.fr (S. Chikh), acampo@emba.uvm.edu (A. Campo).

0142-727X/$ - see front matter © 2006 Published by Elsevier Inc.
doi:10.1016/j.ijheatfluidflow.2006.05.003

Nomenclature

c_p	specific heat, J/kg K
Da	Darcy number, $K/(\varepsilon D^2)$
D	diameter cylinder, m
e_p^*	non-dimensional porous layer thickness, e_p/D
g	gravity acceleration, m/s^2
k	thermal conductivity, W/m K
K	permeability, m^2
Nu	local Nusselt number
$\overline{Nu}$	average Nusselt number
P	pressure, N/m^2
Pr	Prandtl number, ν/α
Ra	Rayleigh number, $g\beta(T_W - T_\infty)D^3/(\nu\alpha)$
Ra^*	modified Rayleigh number, $Ra\,Da/R_c$
R_c	thermal conductivity ratio, k_e/k
T	temperature, °C
u	tangential velocity, m/s
v	radial velocity, m/s
r	radial coordinate, m

Greek symbols

α	thermal diffusivity, m^2/s
β	thermal dilatation coefficient, 1/K
δ_T	thickness of the thermal boundary layer, m
ε	porosity
μ	dynamic viscosity, kg/m s
ν	cinematic viscosity, m^2/s
θ	non-dimensional temperature
ψ	non-dimensional stream function
ρ	density, kg/m^3
φ	tangential coordinate, rd

Subscripts

e	effective
f	fluid
p	porous

Superscript

*	non-dimensional variable

($Pr = 7$ and $0.12 \leqslant Ra \leqslant 70$). Wang et al. (1991) assumed that the surface temperature of the cylinder suddenly jumped to a higher temperature ($Pr = 0.7$ or 7.01 and $10^{-1} \leqslant Ra \leqslant 2 \times 10^7$). Lee and Lin (1997) studied the transient conjugate heat transfer relating the heat conduction inside a solid body of arbitrary shape and the natural convection around the solid. Their numerical results showed that at the very beginning of the cooling process, heat conduction is the prevailing heat transfer mode ($Pr = 7$ and $Ra = 10^7$ or 10^8). Subsequently, multiple plumes arise from the top surface of the solid body due to the particular geometry. The plumes grow up and eventually merge into a single one, which becomes unstable. Thereafter, the decay of natural convection heat transfer reduces the strength of the plume. Recently, Misumi et al. (2003) visualized the flow field of air around a cylinder heated with uniform heat flux. Their experimental results showed that three-dimensional flow separation occurs first in the trailing zone of the cylinder when the Rayleigh number, based on the diameter and the wall heat flux, exceeds 3.5×10^9, and the separation points shift upstream with increasing Rayleigh number. These separations become the trigger to the turbulence transition and turbulent flow appears downstream of the separation at higher Rayleigh number. The experiments also revealed that the local Nusselt number in the laminar boundary layer region increases proportionally to $Ra^{0.2}$. The values increased markedly from the laminar to the transition and turbulent regimes. Correlation equations for average Nusselt number were proposed. They give 15–20% smaller values than those estimated from previous empirical equations (McAdams, 1954, Morgan, 1975, Churchill and Chu, 1974) in the range of the Rayleigh number from 3.5×10^9 to 10^{11}.

Flow in porous media is governed by the empirical Darcy law at weak permeability. However, the inertia and boundary terms must be included at high permeability. The numerical results of Kaviany (1986) showed that the non-Darcian effects reduce the heat transfer rate in porous media confined between two concentric and horizontal cylinders. Merkin (1979) used the Darcy model and the Boundary layer approximations to determine the similarity solution for natural convection problem around a cylinder or a sphere embedded in a porous medium with constant porosity. He showed that the local heat transfer is more important around the sphere at high modified Rayleigh number. The same approach has been adopted by Cheng (1985) that proposed a theoretical correlation for the average Nusselt number in the case of a horizontal isothermal cylinder ($\overline{Nu} = 0.565Ra^{*0.5}$). Fand et al. (1986) considered a porous medium constituted with glass spheres of different sizes. Their experimental measurements of the average Nusselt number were higher than those predicted by theoretical computations (Cheng, 1985). Hsiao et al. (1992) studied the problem of the transient natural convection around a horizontal cylinder in an enclosed porous medium. Non-Darcian effects were taken into consideration in momentum equations, while thermal dispersion effect is accounted for in the energy equation. The wall effect on porosity is approximated by an exponential function. The enclosed porous medium is considered as infinite if the outer boundary is localized at 22.2 times the cylinder diameter. The non-uniform porosity effect tends to increase the temperature gradient adjacent to the wall while the thermal dispersion effect increases the thermal conductivity. Both these effects result in the enhancement of surface heat flux. Finally, the numerical results were in good

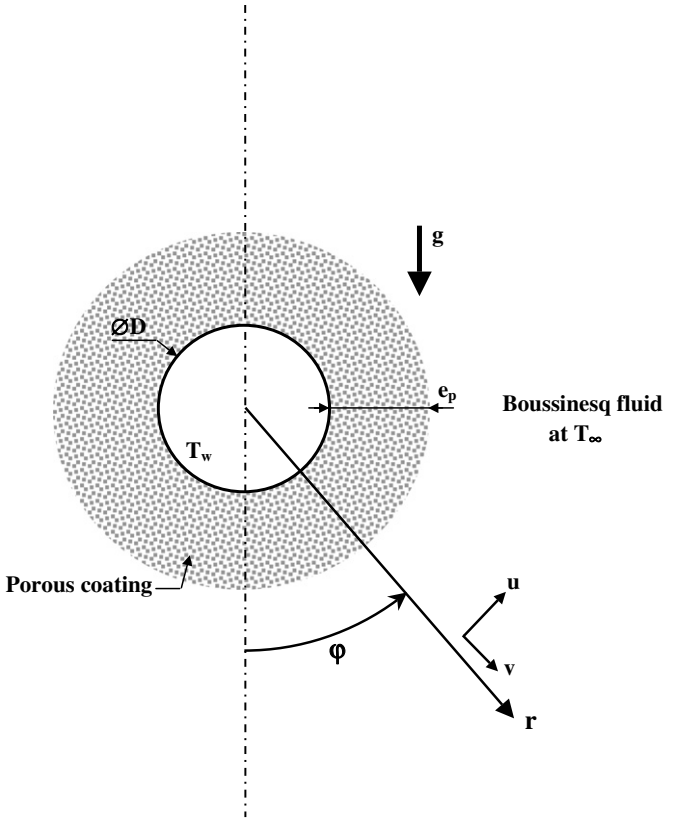

Fig. 1. Schematic of the computation domain.

agreement with the experimental results of Fand et al. (1986).

The present work analyzes the flow and the heat transfer by a 2D laminar natural convection in steady state regime about a horizontal isothermal circular cylinder with a constant temperature T_W and a diameter D. The cylinder placed in air with a temperature T_∞ ($T_\infty < T_W$) is coated by a fibrous layer of thickness e_p, permeability K and effective thermal conductivity k_e, as reported in Fig. 1. The physical domain is not limited by the permeable outer face of the porous coating, but by a fictitious boundary at infinity ($r = R_\infty$). According to the properties of the porous coating, one will determine the appropriate conditions to minimize thermal losses for an efficient insulation or to enhance the heat transfer.

2. Mathematical formulation

The flow and the heat exchange around the cylinder are governed by conservative equations of mass, momentum and energy. Assuming flow symmetry about the vertical centerline $\varphi = 0$, we consider half of the physical domain for computations ($0 \leqslant \varphi \leqslant 180$). The saturated porous medium is assumed homogeneous and isotropic. The solid matrix is in local thermal equilibrium with the fluid. The flow in the porous region is modelled by the macroscopic equations including the microscopic viscous effects represented by the Darcy terms (Vafai and Tien, 1981). The physical properties, evaluated at $T_0 = (T_W + T_\infty)/2$, are considered constant except for density which varies with temperature in the buoyancy terms (Boussinesq approximation).

With these assumptions, the governing equations are written as follows:

$$\frac{\partial}{\partial r}(rv) + \frac{\partial u}{\partial \varphi} = 0 \tag{1}$$

$$\frac{\partial}{\partial r}\left(\rho rvv - \mu r\frac{\partial v}{\partial r}\right) + \frac{\partial}{\partial \varphi}\left(\rho uv - \mu\frac{\partial v}{r\partial \varphi}\right) = -r\frac{\partial P}{\partial r} - \rho\beta(T - T_\infty)g\cos(\varphi)r + \rho\frac{u^2}{r}r - \mu\left(\frac{v}{r^2} + \frac{2}{r^2}\frac{\partial u}{\partial \varphi}\right)r - \frac{\varepsilon\mu}{K}vr \tag{2}$$

$$\frac{\partial}{\partial r}\left(\rho rvu - \mu r\frac{\partial u}{\partial r}\right) + \frac{\partial}{\partial \varphi}\left(\rho uu - \mu\frac{\partial u}{r\partial \varphi}\right) = -r\frac{\partial P}{r\partial \varphi} + \rho\beta(T - T_\infty)g\sin(\varphi)r - \rho\frac{vu}{r}r - \mu\left(\frac{u}{r^2} - \frac{2}{r^2}\frac{\partial v}{\partial \varphi}\right)r - \frac{\varepsilon\mu}{K}ur \tag{3}$$

$$\frac{\partial}{\partial r}\left(\rho c_p rvT - k_e r\frac{\partial T}{\partial r}\right) + \frac{\partial}{\partial \varphi}\left(\rho c_p uT - k_e\frac{\partial T}{r\partial \varphi}\right) = 0 \tag{4}$$

Darcy terms represented by $\frac{\varepsilon\mu}{K}ur$ and $\frac{\varepsilon\mu}{K}vr$ appear in the porous region where the dynamic viscosity is assumed equal to air viscosity. The non-Darcian terms are included in the present formulation. A deep analysis showed that these terms have a significant importance under certain conditions. Accounting for these terms shows a deviation from the Darcy model that may exceed 50% relatively to the average Nusselt number as reported in Fig. 2. By setting the permeability equals to infinity, Eqs. (2) and (3) become the Navier–Stokes equations in the fluid region.

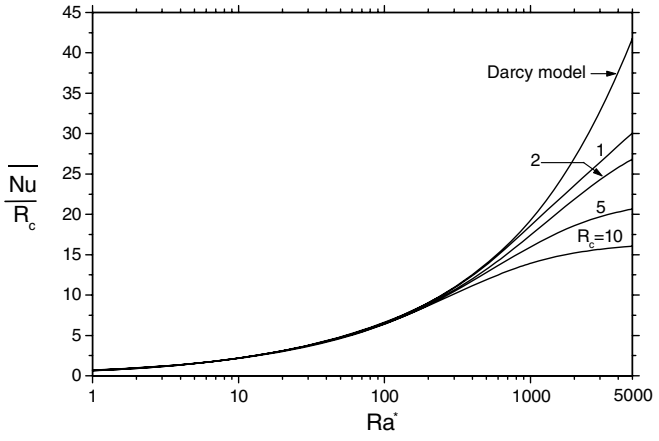

Fig. 2. Non-Darcian effects on heat transfer around a cylinder in infinite porous medium.

After introducing the dimensionless variables defined in the following:

$$r^* = \frac{r}{D}, \quad u^* = \frac{u}{(\alpha/D)}, \quad v^* = \frac{v}{(\alpha/D)},$$
$$P^* = \frac{P}{\rho(\alpha/D)^2}, \quad \theta = \frac{T - T_\infty}{T_W - T_\infty}$$

The governing equations can be written as:

$$\frac{\partial}{\partial r^*}(r^* v^*) + \frac{\partial u^*}{\partial \varphi} = 0 \tag{5}$$

$$\frac{\partial}{\partial r^*}\left(r^* v^* v^* - Pr\, r^* \frac{\partial v^*}{\partial r^*}\right) + \frac{\partial}{\partial \varphi}\left(u^* v^* - Pr \frac{\partial v^*}{r^* \partial \varphi}\right) = -r^* \frac{\partial P^*}{\partial r^*} - RaPr\theta \cos(\varphi) r^* + \frac{u^{*2}}{r^*} r^* - Pr\left(\frac{v^*}{r^{*2}} + \frac{2}{r^{*2}} \frac{\partial u^*}{\partial \varphi}\right) r^* - \frac{Pr}{Da} v^* r^* \tag{6}$$

$$\frac{\partial}{\partial r^*}\left(r^* v^* u^* - Pr\, r^* \frac{\partial u^*}{\partial r^*}\right) + \frac{\partial}{\partial \varphi}\left(u^* u^* - Pr \frac{\partial u^*}{r^* \partial \varphi}\right) = -r^* \frac{\partial P^*}{r^* \partial \varphi} + RaPr\theta \sin(\varphi) r^* - \frac{v^* u^*}{r^*} r^* - Pr\left(\frac{u^*}{r^{*2}} - \frac{2}{r^{*2}} \frac{\partial v^*}{\partial \varphi}\right) r^* - \frac{Pr}{Da} u^* r^* \tag{7}$$

$$\frac{\partial}{\partial r^*}\left(r^* v^* \theta - R_c r^* \frac{\partial \theta}{\partial r^*}\right) + \frac{\partial}{\partial \varphi}\left(u^* \theta - R_c \frac{\partial \theta}{r^* \partial \varphi}\right) = 0 \tag{8}$$

The dimensionless groups appearing in these equations constitute the key parameters of the problem (the Rayleigh number $Ra = g\beta(T_W - T_\infty)D^3/(\nu\alpha)$, the Prandtl number $Pr = \nu/\alpha$, the Darcy number $Da = K/(\varepsilon D^2)$, and the thermal conductivity ratio $R_c = k_e/k$) along with the non-dimensional porous layer thickness ($e_p^* = e_p/D$). Outside of the porous medium, the Darcy number tends toward infinity and the ratio R_c is equal to unity.

The boundary conditions in a dimensionless form are:

$$\text{At } r^* = 0.5 \quad \theta = 1, \quad u^* = v^* = 0 \tag{9a}$$

$$\text{At } r^* = R_\infty/D \; u^* = \frac{\partial v^*}{\partial r^*} = 0, \quad \begin{cases} \theta = 0 & 0 \leqslant \varphi \leqslant \varphi_0 \\ \dfrac{\partial \theta}{\partial r^*} = 0 & \varphi_0 \leqslant \varphi \leqslant 180^\circ \end{cases} \tag{9b}$$

$$\text{At } \varphi = 0 \text{ or } \pi \; \frac{\partial \theta}{\partial \varphi} = 0, \quad u^* = \frac{\partial v^*}{\partial \varphi} = 0 \tag{9c}$$

The fluid enters the computational domain (at $r^* = R_\infty/D$) with a uniform temperature $\theta = 0$ in the region $0 \leqslant \varphi \leqslant \varphi_0$ (φ_0 is an angle depending on problem parameters). In the zone $\varphi_0 \leqslant \varphi \leqslant 180$, the fluid is assumed to leave the domain with negligible radial temperature gradient (Kuehn and Goldstein, 1980).

The matching conditions at the interface between the porous region and the fluid region expressed the continuity of the velocity, the shear stress, the temperature and the heat flux. They are given by:

$$u_f^* = u_p^*, \quad v_f^* = v_p^*, \quad P_f^* = P_p^* \tag{10a}$$

$$\frac{\partial u_f^*}{\partial r^*} = \frac{\partial u_p^*}{\partial r^*}, \quad \frac{\partial v_f^*}{\partial r^*} = \frac{\partial v_p^*}{\partial r^*} \tag{10b}$$

$$\theta_f = \theta_p \tag{10c}$$

$$\frac{\partial \theta_f}{\partial r^*} = R_c \frac{\partial \theta_p}{\partial r^*}, \quad \frac{\partial \theta_f}{\partial \varphi} = R_c \frac{\partial \theta_p}{\partial \varphi} \tag{10d}$$

The local Nusselt number is evaluated at the wall of the cylinder in order to quantify the heat losses with respect to the influential parameters (e_p^*, Ra, Da, R_c). It is defined by:

$$Nu(\varphi) = -R_c \left.\frac{\partial \theta}{\partial r^*}\right|_{r^*=0.5} \tag{11}$$

The average Nusselt number is a convenient way of measuring the increase in global heat transfer. It is computed by

$$\overline{Nu} = \frac{1}{\pi} \int_0^\pi Nu(\varphi)\, d\varphi \tag{12}$$

3. Numerical procedure

The set of governing partial differential equations (5)–(8) with the corresponding boundary conditions are discretized by use the control volume method. Staggered grids and SIMPLE algorithm as suggested by Patankar (1980) are adopted to treat the coupling between velocity and pressure fields. A Power law differencing scheme is used to consider the contribution of convection and diffusion in the transport phenomena. The set of obtained algebraic equations are solved using a combination between the tridiagonal matrix algorithm (TDMA) and the Gauss–Seidel point iterative method associated with an underrelaxation. The solution is assumed to be reached during the iterative process, when the maximum relative error on the dependant variable ϕ (velocity components, pressure and temperature) is less than 10^{-3},

$$\max\left|\frac{\phi - \phi^*}{\phi^*}\right| < 0.001$$

ϕ^* is evaluated at previous iteration. In addition, the maximum allowable absolute residue on continuity equation must be less than 10^{-10}.

A grid sensitivity analysis is first undertaken. A number of 110×200 nodes in φ and r respectively are considered. The radial direction receives 100 nodes uniformly distributed on a thickness of 0.05 around the cylinder; the other 100 nodes are arranged according to a power law. The analysis shows that a finer grid does not affect much the accuracy at the expense of a larger computation time. The response of the average Nusselt number to a change in the grid size for different thicknesses shows a maximum difference less than 0.4%.

The position of the outer boundary of the computation domain has an effect on the results if it is not set far enough from the surface of the cylinder (Kuehn and Goldstein, 1980). It is closer to the cylinder when the Rayleigh number (Ra) or the modified Rayleigh number ($Ra^* = Ra\, Da/R_c$)

increases. Table 1 illustrates this effect on the average Nusselt number, less than 0.14% in difference is obtained.

Prior to results discussion, our computer code is validated by a comparison of our simulation results with previously published ones. The variation of the average Nusselt number is reported in Table 2. The comparison shows an excellent agreement between our results and the ones of Kuehn and Goldstein (1980). Less than 4% in maximum difference is obtained in the range $10^3 \leqslant Ra \leqslant 10^7$. However, there is less than 16.3% while comparing with results obtained by the empirical correlation of Churchill and Chu (1974). The local Nusselt number is plotted in Fig. 3 for $Ra = 10^5$. We observe a good agreement with the results of Kuehn and Goldstein (1980).

Table 1
Effect of the outer boundary position of the computation domain on the average Nusselt number (110×200 nodes, $Ra = 10^8$, $Da = 10^{-5}$, $R_c = 1$)

e_p^*	$\overline{Nu}$			
	$R_\infty/D = 10.5$	$R_\infty/D = 8$	$R_\infty/D = 5.5$	% Difference
0	40.9534	40.9463	40.9365	0.017–0.024
0.01	32.9314	32.9299	32.9263	0.005–0.011
0.1	17.8164	17.8160	17.8146	0.002–0.008
1	17.8689	17.8684	17.8678	0.003
∞	18.0075	17.9924	17.9677	0.084–0.137

Table 2
Comparison with published results for heat transfer about a cylinder without porous coating

Ra	$\overline{Nu}$				
	Numerical results (Kuehn and Goldstein, 1980)	Empirical correlation (Churchill and Chu, 1974)	Present study	% Difference	
				Kuehn and Goldstein (1980)	Churchill and Chu (1974)
10^3	3.09	2.560	2.9754	3.71	16.23
10^4	4.94	4.272	4.7638	3.57	11.51
10^5	8	7.317	7.8897	1.38	7.832
10^6	13.52	12.731	13.4095	0.82	5.331
10^7	23.32	22.359	23.2747	0.19	4.096

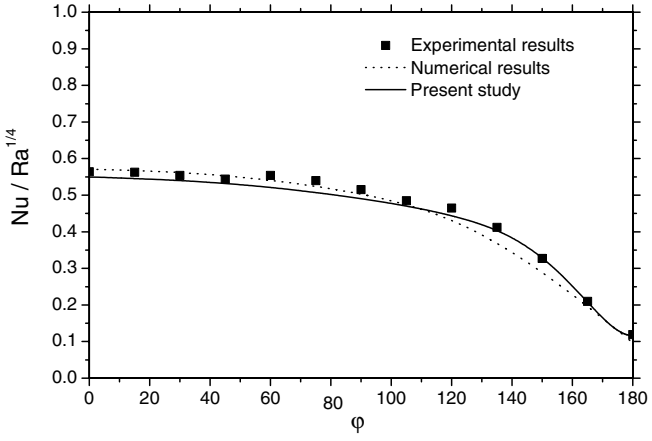

Fig. 3. Comparison with published results of Kuehn and Goldstein (1980) for heat transfer around a cylinder in a clear fluid ($Pr = 0.7$, $Ra = 10^5$).

4. Results and discussion

Computations were conducted for $Pr = 0.7$ and $Ra = 10^8$. The obtained predictions are organized in two parts. First, we consider fibrous or porous materials with relatively small thermal conductivity ratio $R_c \leqslant 2$, intended for insulation purpose. In the second part, we analyze porous media with high thermal conductivity ratio that can be used as an alternative for heat transfer enhancement.

4.1. Thermal insulation

To analyze thermal insulation, we consider materials with rather low effective thermal conductivity ($R_c = 1$). Then, we investigate materials with slightly higher conductivity ratio (up to $R_c = 2$). In order to quantify the heat transfer rate and heat losses from the hot cylinder, let us first present the velocity and temperature profiles. Fig. 4a and b display the velocity profiles at different φ positions. The porous material is characterized by its thickness ($e_p^* \geqslant 0.1$) and its permeability expressed by the Darcy number ($Da = 10^{-5}$ and 10^{-8}). For relatively high permeability, $Da = 10^{-5}$ (Fig. 4a), two hydrodynamic boundary layers develop: one over the cylinder and one over the porous coating. In the lower region, the velocity is higher within the porous layer except for a very thin coating ($e_p^* = 0.1$) where the fluid is accelerated outside the porous region in the upper zone of the cylinder at $\varphi = 135°$ and $\varphi = 170°$ in Fig. 4a. Darcy effects represent the importance of viscous forces due to friction on the pore walls. Being more intense for a weakly permeable porous medium ($Da = 10^{-8}$), Fig. 4b, they balance the buoyancy forces and reduce consequently the flow velocity which vanishes within the porous layer. This leads to a situation of conduction within the porous material with no fluid motion. Furthermore, the dynamic boundary layer on the cylinder is disrupted with the reduction of the porous layer thickness below the limit of the boundary layer development in an infinite porous medium. This reduction can induce greater maximum velocities mainly at top of the cylinder in the fluid region compared to the porous region, because of progressively increasing action of buoyancy forces. On the other hand if one considers a weakly permeable porous material ($Da = 10^{-8}$), there would rather be apparition of only one dynamic boundary layer in the fluid region where the maximum velocity varies inversely with the thickness e_p^*, Fig. 4b.

Temperature profiles are plotted in Fig. 5a and b for the same study parameters considered previously. The temperature distribution shows a decay in the radial direction whatever are the properties of the porous medium (e_p^* and Da) (Kuehn and Goldstein, 1980; Cheng, 1985;

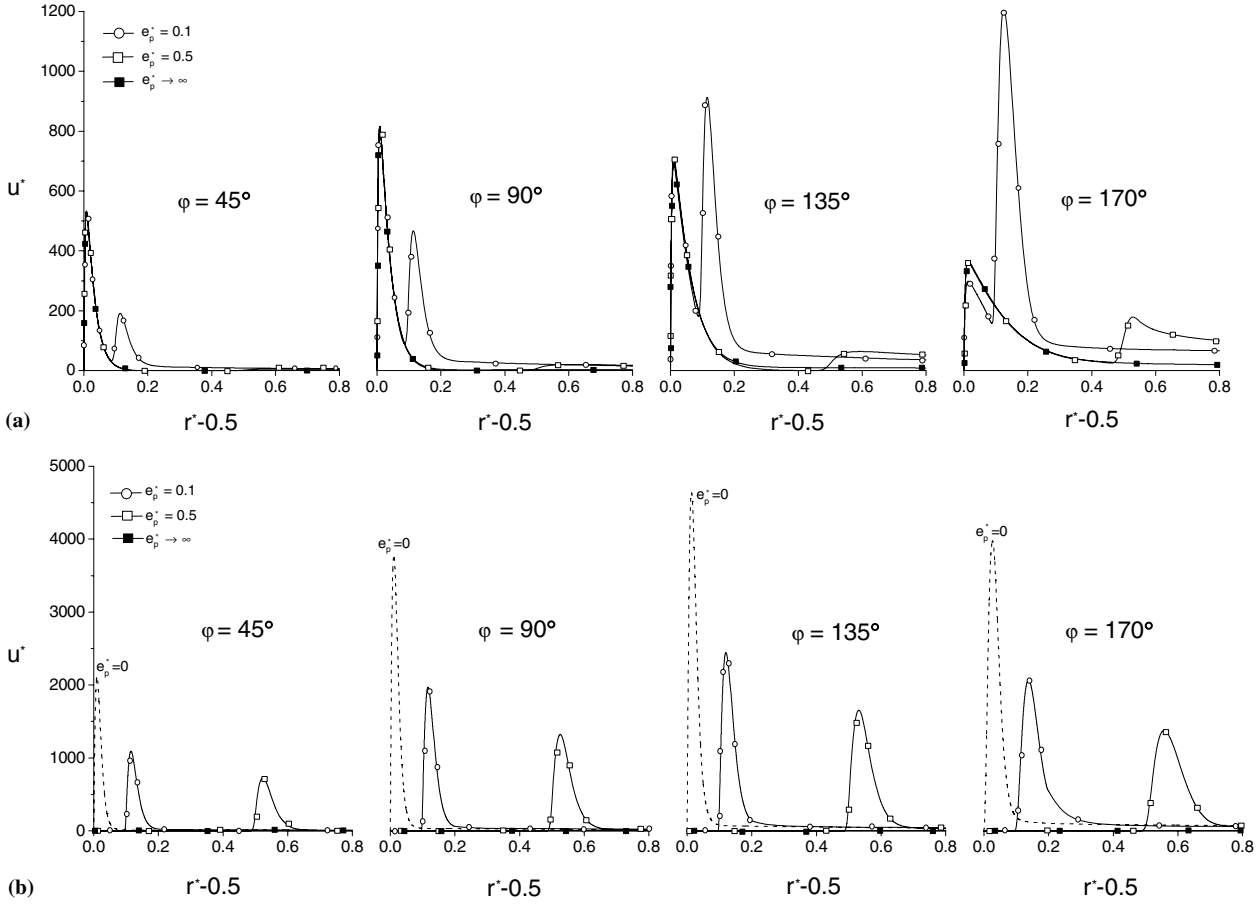

Fig. 4. Velocity profiles ($R_c = 1$): (a) $Da = 10^{-5}$ and (b) $Da = 10^{-8}$.

Fand et al., 1986). Only one thermal boundary layer develops on the cylinder from its low extreme point. It is followed at top of the cylinder by a thermal plume where the heat transfer is less important. Indeed, as depicted in Fig. 5, the temperature level increases and the radial temperature gradient decreases while browsing the cylinder from the bottom to the top in the azimuthal direction. For finite thicknesses of the coating, one can notice the great effect of Da on temperature gradient at the interface porous-fluid at the position $\varphi = 180°$. For $Da = 10^{-5}$, Fig. 5a, the temperature gradient increases at the interface, whereas it decreases for $Da = 10^{-8}$ as clearly illustrated in Fig. 5b for the case of $e_p^* = 0.1$ or 0.5.

One completes the thermal study by the analysis of the thermal boundary layer (TBL) thickness, as shown in Fig. 6a–c. From the computational point of view, the limit of the thermal boundary layer is an isotherm line of temperature $\theta = 0.01$. The TBL δ_T increases with the φ angle and it is subject to a more important variation in the thermal plume zone at top of the cylinder ($\varphi \geqslant 170°$). The same evolution is obtained when the porous layer becomes thicker or less permeable. For $Da = 10^{-5}$, the TBL is very thin, and with small thicknesses (e_p^* starting from 0.1 or 0.2), the coating may acts as an infinite porous layer except in the plume zone. However, with less permeable materials, Fig. 6b and c, a porous coating of thickness over 2, for $Da = 10^{-7}$ for example, is needed in order to act as an infinite one particularly in the lower part of the cylinder.

To illustrate and emphasize the previous discussion, streamlines and isotherms are presented in Figs. 7 and 8 for different thicknesses of the coating and for different values of Da. These figures confirm the results cited by examining the magnitude of the stream function or the isotherms. Dynamic and thermal boundary layers develop on the cylinder without the coating (Fig. 7a) or embedded in an infinite porous medium (Fig. 7b). The boundary layers are thicker in the second case where the magnitude of velocity is smaller. The boundary layer is followed by a thermal plume in the upper zone of the cylinder. When the porous layer has a finite thickness, another dynamic boundary layer develops on the porous coating for small thicknesses (Fig. 7c). However, this second boundary layer is not displayed for a higher thickness (Fig. 7d). With regard to temperature variation, the thermal boundary layer is localized in the porous medium when this latter is thick (Fig. 7d) and it extends to the fluid domain when the porous medium is thin (Fig. 7c). This is due to the buoyant forces which still act beyond the porous limit for the permeability represented.

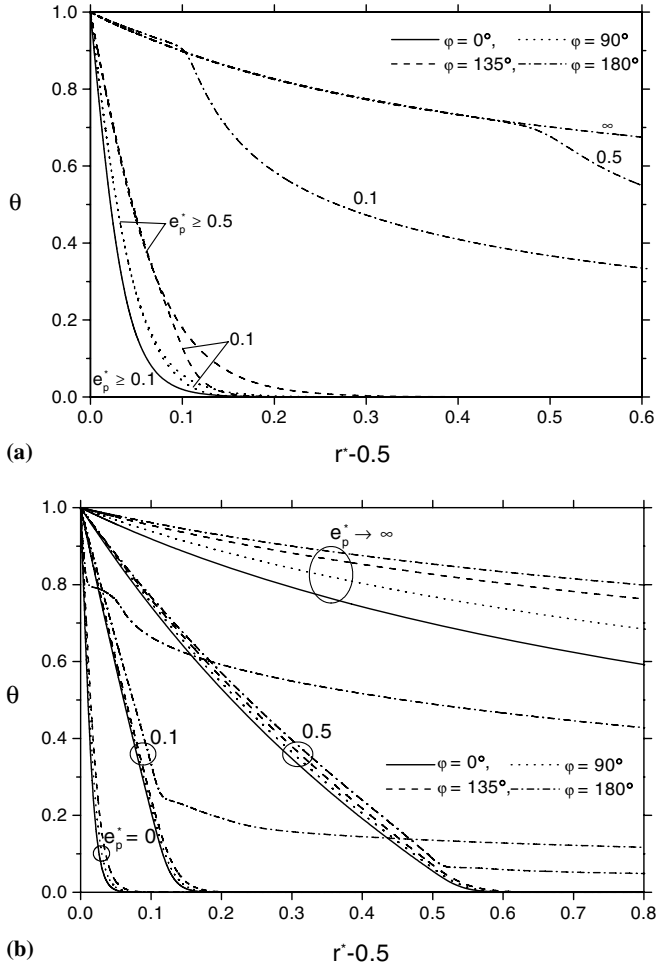

Fig. 5. Temperature profiles ($R_c = 1$): (a) $Da = 10^{-5}$ and (b) $Da = 10^{-8}$.

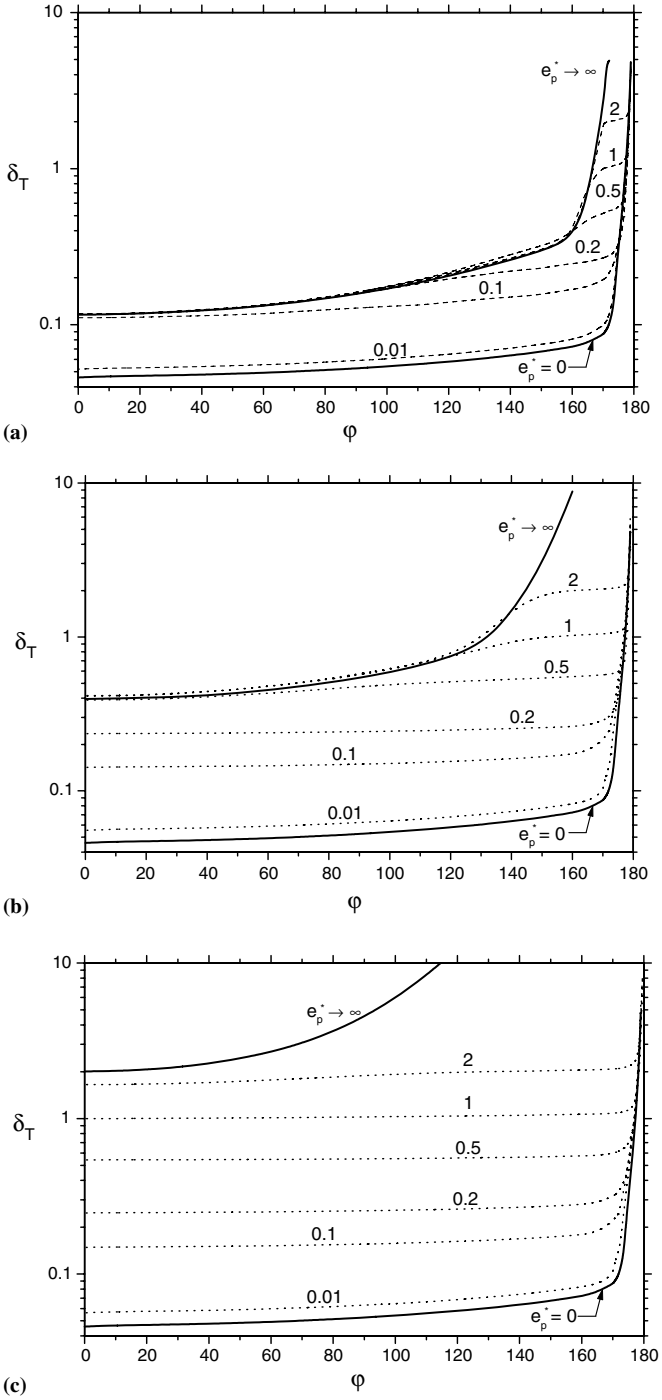

Fig. 6. Variation of the thermal boundary layer thickness around the cylinder ($R_c = 1$): (a) $Da = 10^{-5}$, (b) $Da = 10^{-6}$ and (c) $Da = 10^{-7}$.

The effect of the Darcy number on the streamlines and isotherms distribution is shown in Fig. 8 for a porous layer of thickness $e_p^* = 1$. The thermal plume extends to 13° from the vertical centreline starting from the top ($Da = 10^{-5}$). The heat losses are more important in the boundary layer than in the thermal plume. Indeed, the boundary layer becomes thicker and extends to a wider region as Da decreases. The inflow and outflow limit in the porous layer are fixed at higher angle when the porous material is less permeable (for the outflow $\varphi = 115°$ for $Da = 10^{-7}$ and $\varphi = 95°$ for $Da = 10^{-8}$). However, the thermal boundary tends to disappear for $Da \leqslant 10^{-7}$. Thermal convection becomes negligible and thermal conduction is then the main mode of heat transfer.

The local heat losses from the cylinder are quantified by the local Nusselt number which is plotted versus φ angle. Fig. 9a displays the effect of Darcy number for a porous layer with $e_p^* = 0.5$ and $R_c = 1$. The local Nusselt number presents a decreasing trend from the bottom to the top of the cylinder in which the variation is higher because of the thermal plume formation (Kuehn and Goldstein, 1980; Farouk and Guceri, 1981; Cheng, 1985; Fand et al., 1986; Hsiao et al., 1992). This is mainly due to heating of air while rising. The effect of Da is negligible either for very permeable porous material ($Da \geqslant 10^{-3}$) or weakly permeable material ($Da \leqslant 10^{-8}$). In the first case, the local variation of the heat transfer is weak in the boundary layer, but decreases abruptly and then increases in the thermal plume region because of the air recirculation obtained at top of the cylinder for high Rayleigh number ($Ra = 10^8$) (Misumi et al., 2003). In the second case, the variation of Nu is negligible. It tends to the case of a solid coating

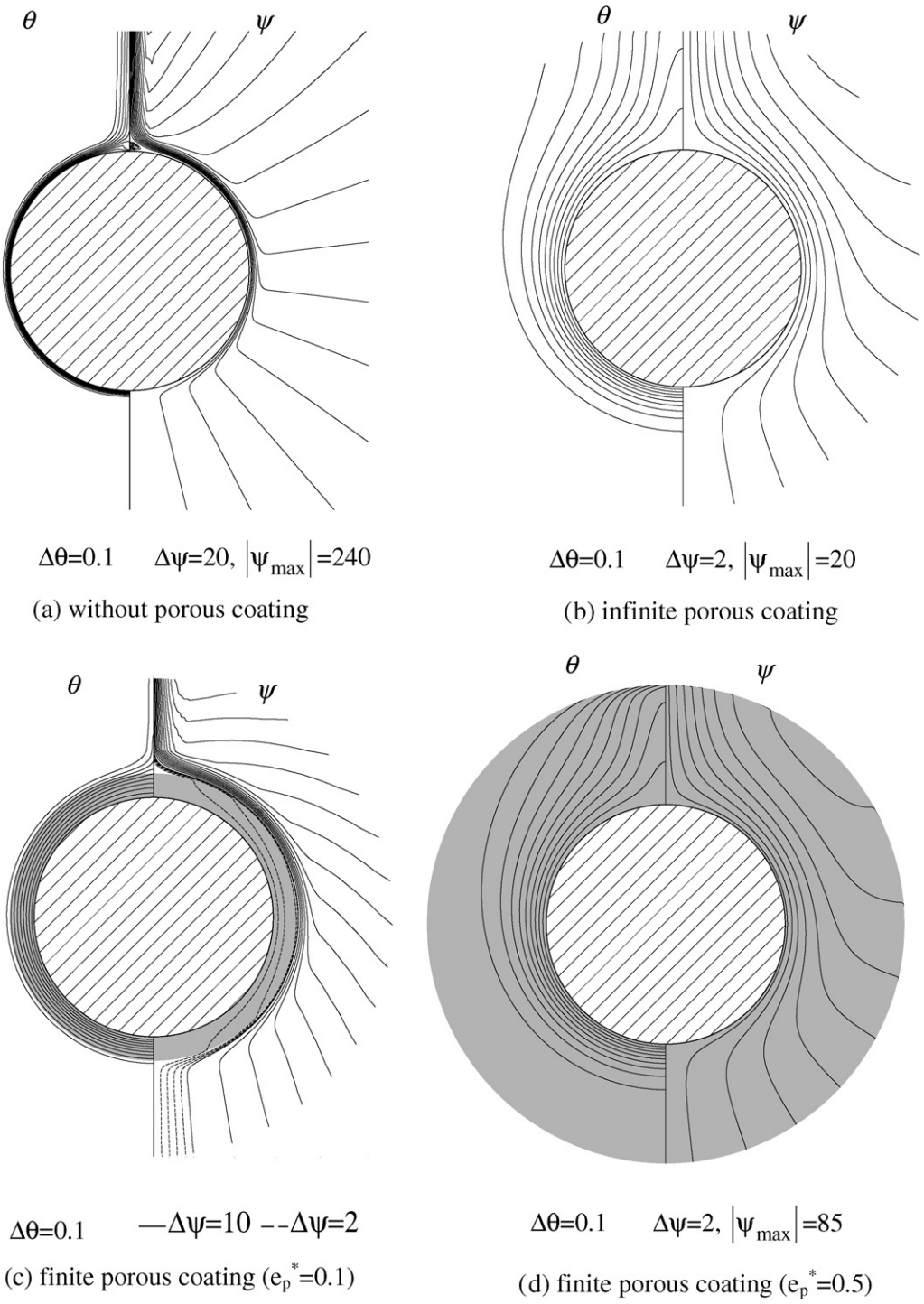

Fig. 7. Streamlines and isotherms versus porous layer thickness ($R_c = 1$, $Da = 10^{-6}$).

and hence the heat exchange mode is mainly conduction. Decreasing the Darcy number reduces the local heat losses in the thermal boundary layer which become thicker.

The heat losses at different φ positions on the cylinder wall are also influenced by the thickness of the porous coating, as illustrated in Fig. 9b. These effects diminish when the material is more permeable. The distribution of the local Nusselt number is independent of the thickness when this latter is higher than 0.1 for $Da = 10^{-4}$ or is higher than 0.5 for $Da = 10^{-6}$. We found the solution corresponding to the case of infinite porous coating.

The total heat losses from the cylinder are quantified by the computation of the average Nusselt number. The thickness e_p^* and the Darcy number Da constitute the two parameters that affect the global heat transfer as reported in Fig. 10. Thermal insulation of a cylinder covered with

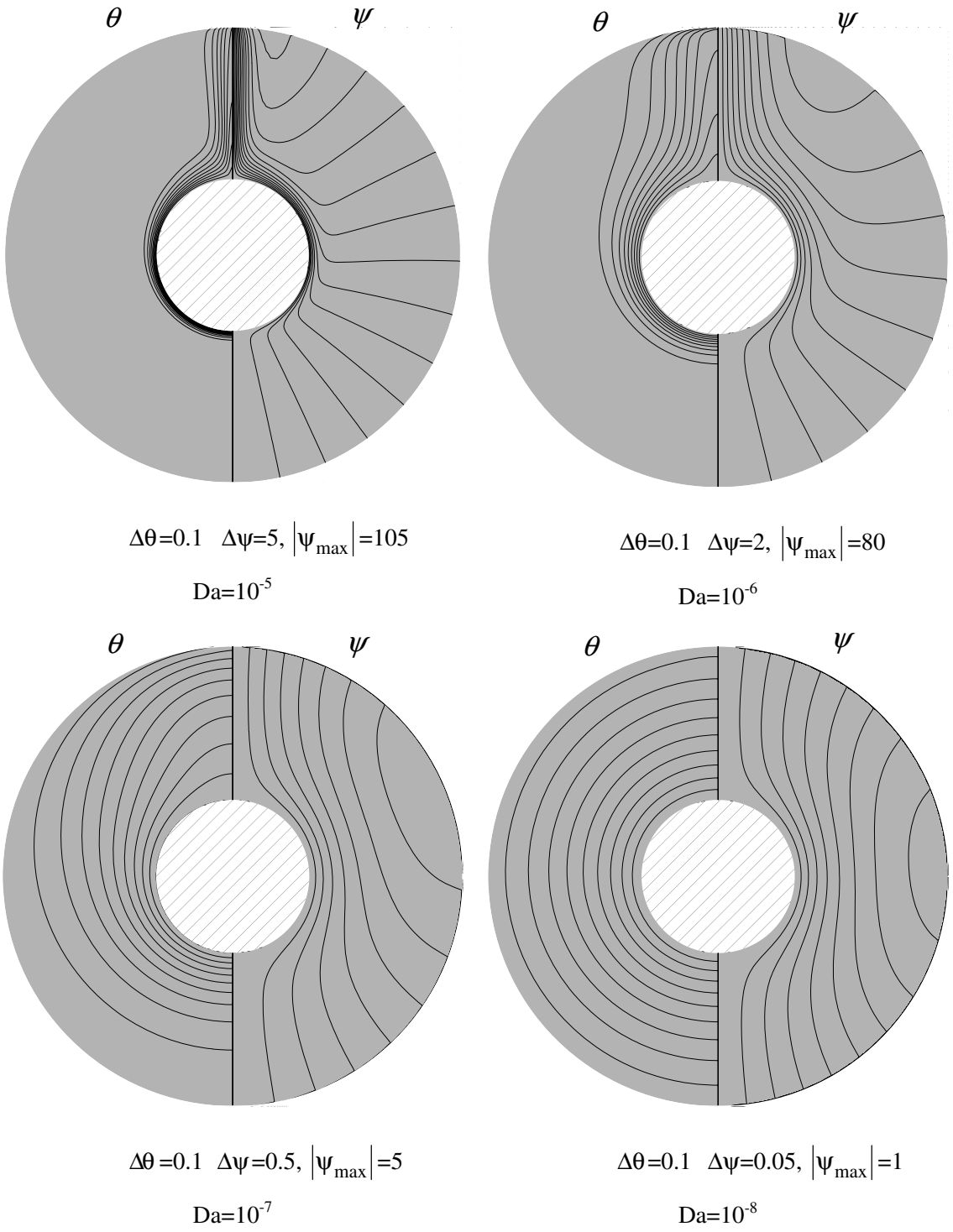

Fig. 8. Streamlines and isotherms versus Darcy number ($e_p^* = 1$, $R_c = 1$).

a porous coating is supposed achieved when the heat losses are reduced compared to the case without porous coating ($e_p^* = 0$). The effect of the permeability (Da) is more important with thicker porous coating. The influence of the thickness shows only at low Da values. At a given Da, increasing the porous coating thickness implies a greater resistance to conduction. Thus, one would say that for thermal insulation if the insulating material is weakly permeable then the thickness should be the optimizing parameter. But, if the insulating material is very permeable, the thickness has less meaning since convection is the main mode of heat transfer. Then an optimal thickness is deduced and is plotted in Fig. 11 for different values of R_c. It varies inversely with Da. Its increasing variation with

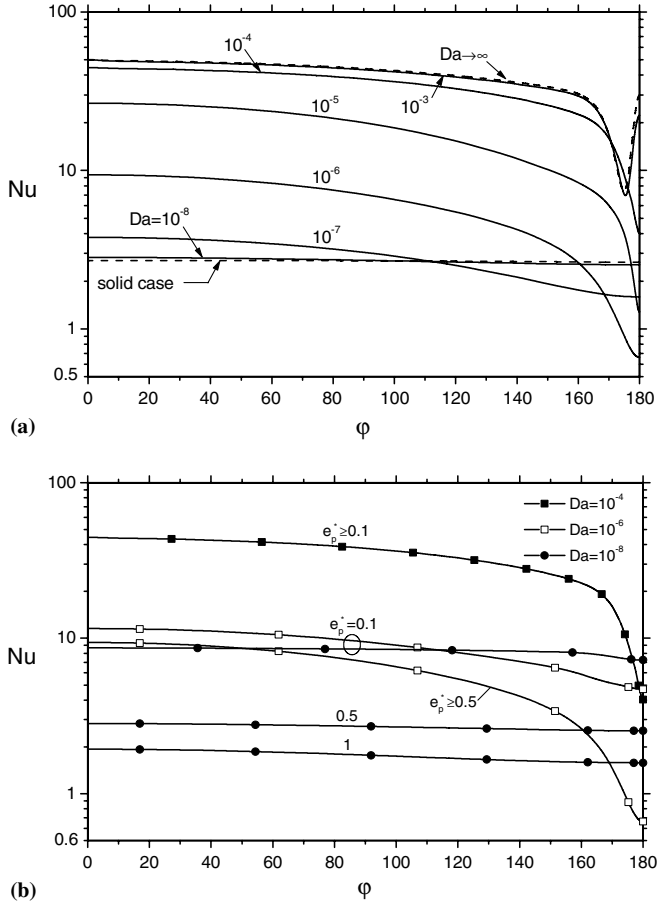

Fig. 9. (a) Effect of Da on local Nusselt number ($e_p^* = 0.5$, $R_c = 1$) and (b) effect of e_p^* on local Nusselt number ($R_c = 1$).

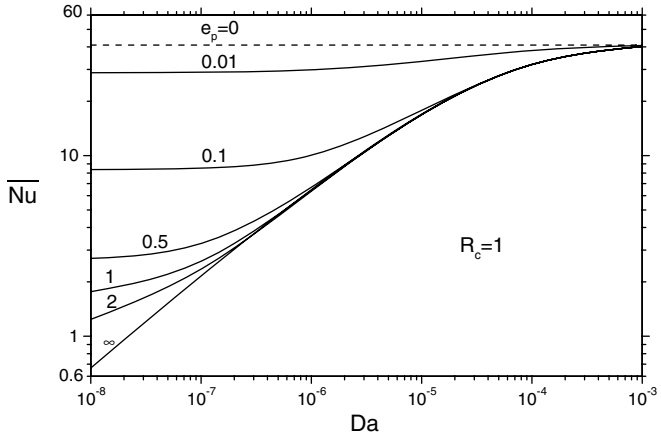

Fig. 10. Average Nusselt number versus Darcy number.

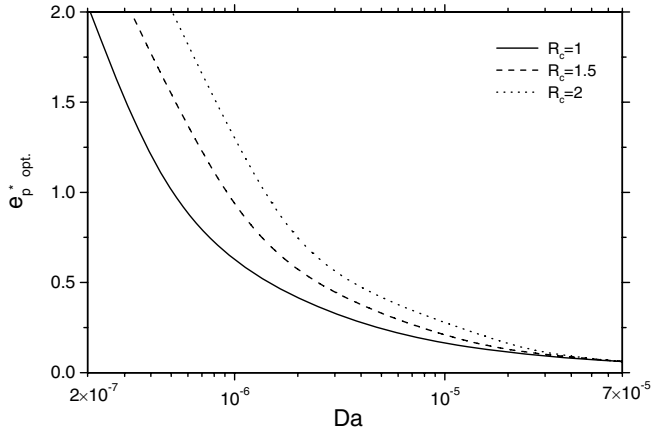

Fig. 11. Optimal porous layer thickness versus Darcy number.

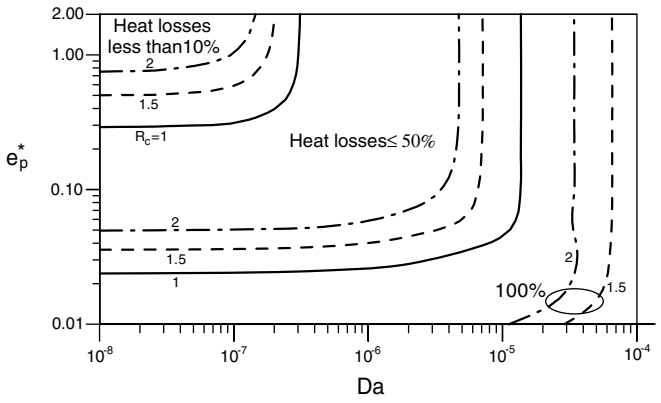

Fig. 12. Heat losses cartography.

R_c reduces at high permeability. For $e_p^* \geqslant e_{p\,opt}^*$, $\overline{Nu}$ converges to the value obtained in the case of infinite porous medium.

Fig. 12 displays a cartography of heat losses percentage. The best insulation of the cylinder corresponds to heat losses less than 10%. This result is obtained when $e_p^* \geqslant 0.3$ and $Da \leqslant 2 \times 10^{-7}$ while considering a porous insulator with $R_c = 1$. When the thermal conductivity ratio R_c increases, then the limit of this range is modified. The thickness limit increases to ensure a greater thermal resistance, while the Darcy number limit decreases to recover more heat transferred by thermal convection. Thus, the best thermal insulation may be designed with a material verifying $e_p^* \geqslant 0.8$ and $Da \leqslant 10^{-7}$. Fig. 13 shows the limit between the Darcy regime and the non-Darcy one for the cases of finite porous coating. The non-Darcian effects are present in the range of $Da \geqslant 10^{-6}$ and $e_p^* \leqslant 0.1$. In addition, the porous material of very small permeability is the seat of heat transfer by conduction. Therefore, the porous structure of the coating material can be assimilated to a solid structure at a certain limit of Da that depends on the thickness e_p^*. This limit is obtained when the average Nusselt number ratio (solid/porous) is equal to 0.95, and gives the range in which the conduction theory may be applied for the thermal insulation design. Whereas, elsewhere the conduction–convection theory associated to the non-Darcy model for $Da \geqslant 10^{-6}$ must be considered. As an illustrative example, with a porous material of $e_p^* = 0.5$, $Da = 10^{-6}$, $R_c = 1.5$ and a cylinder diameter $D = 0.276$ m as well as a temperature difference $(T_W - T_\infty) = 314$ K, the heat losses are estimated at

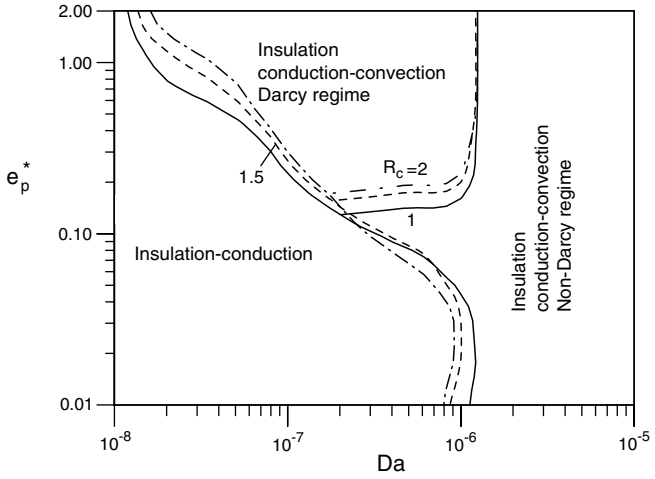

Fig. 13. Non-Darcian effects and limit of the conduction theory application for the insulation design.

161.96 W/m^2 using the conduction theory. Accounting for convection, these losses are amplified and reach 331.15 W/m^2.

4.2. Heat transfer augmentation

Although porous, fibrous or foam materials may generate additional pressure drop, they can be an excellent alternative for heat transfer enhancement because of their interesting specific surface. Indeed, pressure drop is not of great importance in many situations where heat transfer is the main phenomenon of interest. For this purpose, it is worth exploring cases of porous materials with high effective thermal conductivity ($R_c > 2$).

The effect of the thermal conductivity ratio on the thermal boundary layer thickness is examined in Fig. 14 for two values of Darcy number ($Da = 10^{-6}$, 10^{-3}). Fig. 14a shows the case of a porous coating with a slightly low permeability ($Da = 10^{-6}$). The great impact of R_c is clearly depicted for thick porous coatings ($e_p^* \geqslant 1$). Increasing effective thermal conductivity makes the boundary layer thicker and reduces consequently the temperature gradient. For more permeable ($Da = 10^{-3}$) and highly conducting ($R_c = 5$ or 10) porous material, Fig. 14b, the thickness δ_T increases with e_p^*, then reaches a maximum value before it starts declining. The heat transfer from the cylinder without the porous coating is quantified by the average Nusselt number Nu_f. If it is covered with a porous layer, the cylinder is cooled when the thermal losses increase and it is insulated when they decrease. In terms of the heat transfer coefficient, Fig. 15, reports the ratio of the average number with respect to the value of Nu in the clear fluid case. All the curves above the value of 1 represent situations of heat transfer enhancement and below the horizontal dashed line cases of insulation.

The variation of Nu/Nu_f versus the thermal conductivity ratio R_c for a thin porous layer ($e_p^* = 0.01$) is plotted in Fig. 15a. One can notice that very permeable materials

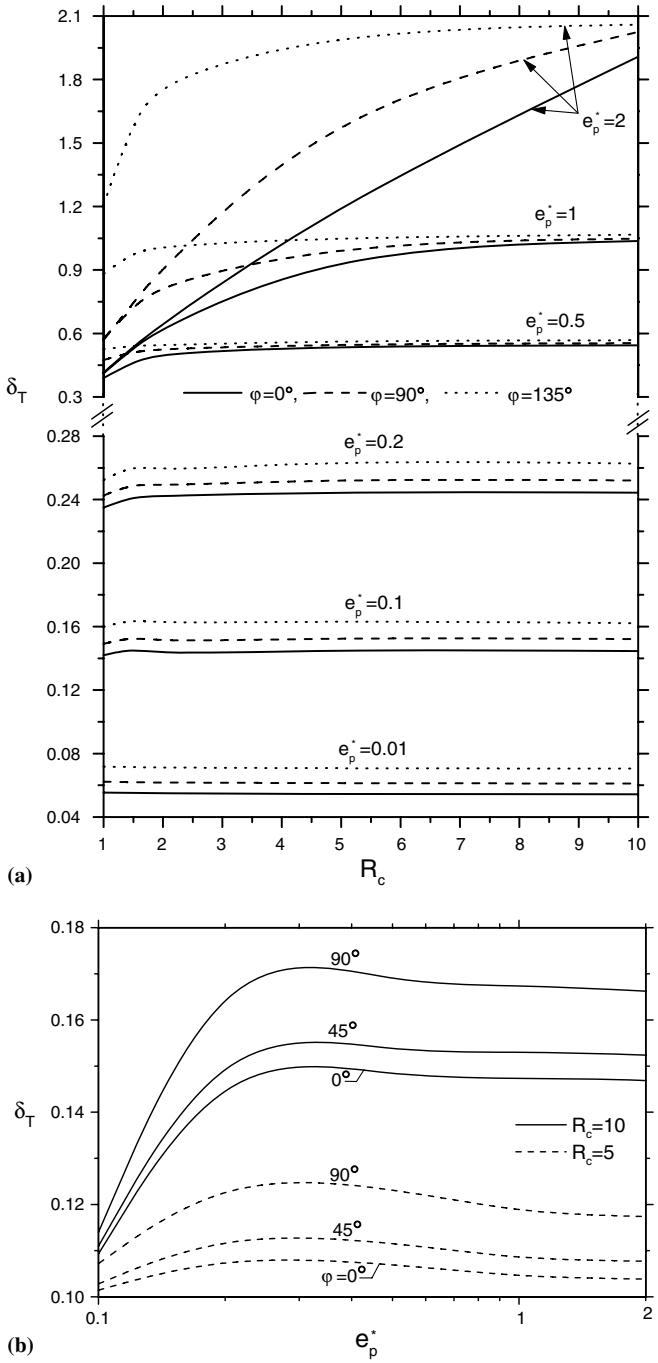

Fig. 14. (a) Effect of R_c on the thermal boundary layer thickness ($Da = 10^{-6}$) and (b) effect of e_p^* on the thermal boundary layer thickness ($Da = 10^{-3}$).

($Da > 10^{-4}$) yield an interesting augmentation in heat transfer coefficient. This is mainly due to their practically small dynamic resistance to the flow and their advantageous thermal conductivity (higher than that of air $R_c > 1$). If the structure of the porous material offers a great dynamic resistance i.e. with less permeable media ($Da \leqslant 10^{-8}$), an excellent effective thermal conductivity is mandatory to achieve heat transfer enhancement. For example, R_c has to be greater than approximately 2.5 for

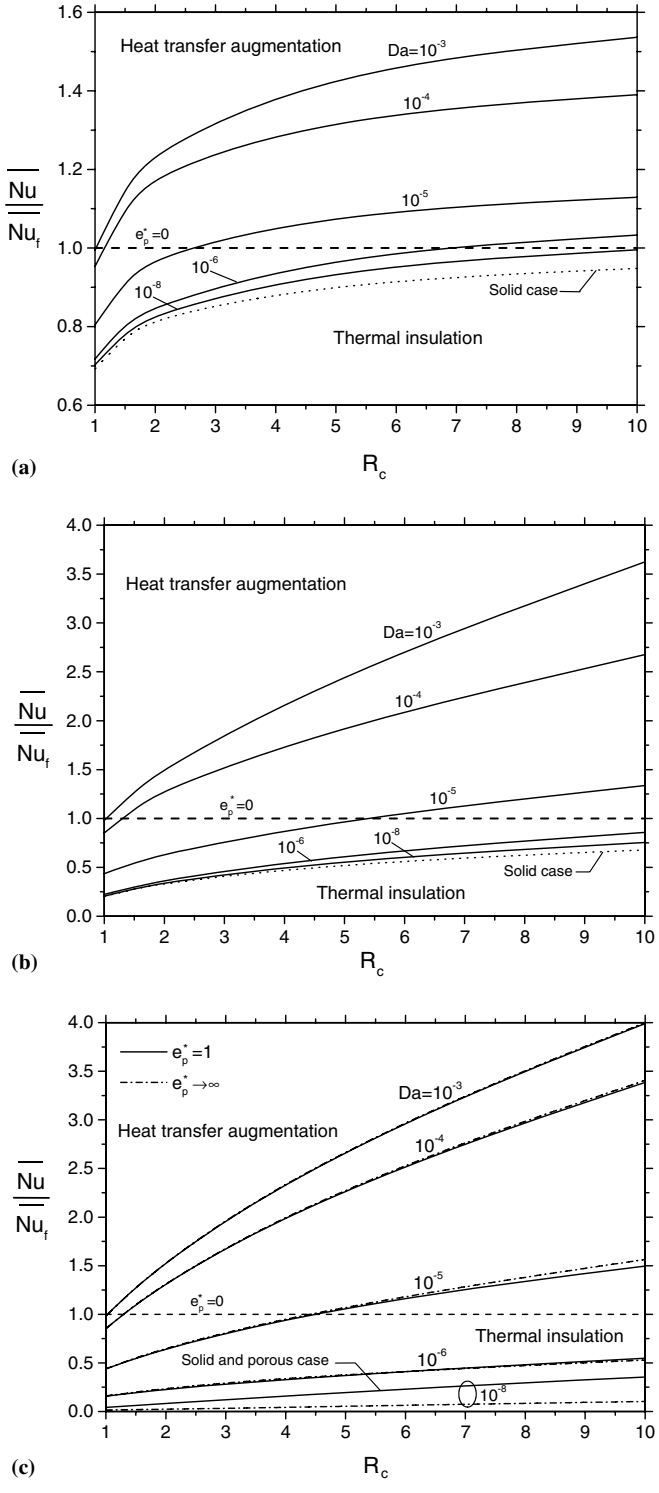

Fig. 15. Effect of R_c on average Nusselt number for different thicknesses: (a) $e_p^* = 0.01$, (b) $e_p^* = 0.1$ and (c) $e_p^* = 1$ and ∞.

$Da = 10^{-5}$ and over 6.5 for $Da = 10^{-6}$. This critical value of R_c increases with decreasing permeability. It may be explained by the fact that a less permeable porous structure means a greater heat transfer resistance due to convection. Thus, we have to reduce the thermal resistance due to conduction by increasing R_c. The limit of R_c value depends on

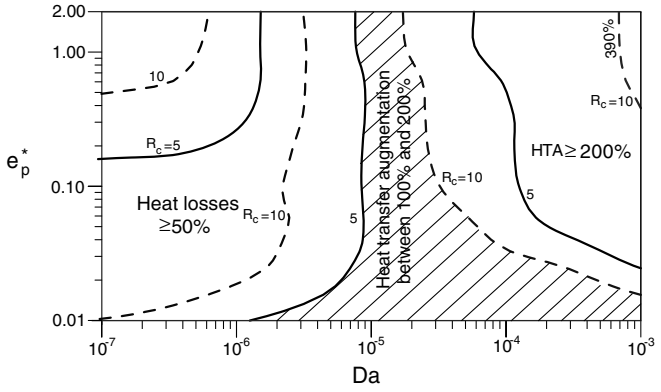

Fig. 16. Optimal conditions for heat transfer enhancement.

the coating thickness as reported in Fig. 15b and c. However, it should be mentioned that it does not vary in a monotonic manner. To illustrate this, let us consider the case of $Da = 10^{-5}$, the limit value of R_c is about 2.5, 5.4 and 4.4 for $e_p^* = 0.01$, 0.1 and 1 respectively. The effect of e_p^* is limited by an optimal value which is much more difficult to reach in the thermal insulation zone for very low permeabilities and high thermal conductivity ratios (Fig. 15c). Thus for $Da = 10^{-5}$, the optimal value is higher than 1 for $R_c = 10$ and between 0.01 and 0.1 for $R_c = 1$. For this reason, the limit of R_c value increases when e_p^* passes from 0.01 to 01 and then decreases for higher values of this parameter. To summarize under what conditions in terms of the porous material properties (permeability, effective thermal conductivity and thickness), Fig. 16 presents a percentage of heat transfer augmentation in comparison with the case of a cylinder in a clear fluid. $Da = 10^{-5}$ constitutes a limit value between reduction and augmentation of heat transfer while using highly conducting porous material ($R_c \geqslant 5$). For heat transfer enhancement design one chooses the region in map corresponding to a percentage higher than 200%. As one can simply choose a porous coating of $e_p^* \geqslant 0.03$, $Da \geqslant 10^{-3}$ and $R_c \geqslant 5$.

5. Conclusion

Flow field and heat transfer by natural convection about a horizontal cylinder with a porous coating is investigated by use of a mathematical model introducing the non-Darcian effects in the porous medium. The Darcy model may be applied in the case of infinite porous coating for $Ra \leqslant 10^8$ and $Da \leqslant 10^{-5}$. The decrease of Ra enhances the non-Darcian effects that can reduce the heat transfer by 39% for $Ra = 10^6$. The numerical results show that if the permeability of a finite porous coating corresponds to a Darcy number greater than 10^{-6}, then one must apply the conduction–convection theory combined to the non-Darcian model. So, the critical thickness of insulation obtained by considering conduction alone is questionable. However, there is also a region of weak velocity in porous layer, which is bounded by a Darcy number limit depending on the porous coating thickness and where the conduc-

tion theory application is sufficient for the thermal insulation design. Furthermore, if the porous material has to be used for heat transfer enhancement purpose, it is suitable to select quite permeable and highly conducting porous media.

References

Cheng, P., 1985. Natural convection in porous media: external flows. In: Kakac, S., Aung, W., Viskanta, R. (Eds.), Natural Convection: Fundamentals and Applications. Martinus Nijhoff, The Hague, The Netherlands, pp. 453–475.

Churchill, S.W., Chu, H.S., 1974. Correlation equation for laminar and turbulent free convection from horizontal cylinder. Int. J. Heat Mass Transfer 18, 1049–1053.

Fand, R.M., Steinberger, T.E., Cheng, P., 1986. Natural convection heat transfer from a horizontal cylinder embedded in a porous medium. Int. J. Heat Mass Transfer 29, 119–133.

Farouk, B., Guceri, S.I., 1981. Natural convection from a horizontal cylinder-laminar regime. ASME J. Heat Transfer 103, 522–527.

Hsiao, S., Cheng, P., Chen, C., 1992. Non-uniform porosity and thermal dispersion effects on natural convection about a heated horizontal cylinder in a enclosed porous medium. Int. J. Heat Mass Transfer 35, 3407–3418.

Kaviany, M., 1986. Non-Darcian effects on natural convection in porous media confined between horizontal cylinders. Int. J. Heat Mass Transfer 29 (10), 1513–1519.

Kuehn, T.H., Goldstein, R.J., 1980. Numerical solution to the Navier–Stokes equations for laminar natural convection about a horizontal isothermal circular cylinder. Int. J. Heat Mass Transfer 23, 971–979.

Lee, S.L., Lin, D.W., 1997. Transient conjugate heat transfer on a naturally cooled body of arbitrary shape. Int. J. Heat Mass Transfer 40 (9), 2133–2145.

McAdams, W.H., 1954. Heat Transmission, third ed. McGraw-Hill, pp. 175–177.

Merkin, J.H., 1979. Free convection boundary layers on axisymmetric and two-dimensional bodies of arbitrary shape in saturated porous medium. Int. J. Heat Mass Transfer 22, 1461–1462.

Misumi, T., Suzuki, K., Kitamura, K., 2003. Fluid flow and heat transfer of natural convection around large horizontal cylinders: experiments with air. Heat Transfer – Asian Res. 32 (4).

Morgan, V.T., 1975Advances in Heat Transfer, vol. 11. Academic Press, pp. 199–210.

Patankar, S.V., 1980. Numerical Heat Transfer and Fluid Flow. McGraw-Hill, Hemisphere, Washington, DC.

Qureshi, Z.H., Ahmed, R., 1987. Natural convection from a uniform heat flux horizontal cylinder at moderate Rayleigh numbers. Numer. Heat Transfer 11, 199–212.

Song, Y.W., 1989. Numerical solution of transient natural convection around a horizontal wire. ASME J. Heat Transfer 111, 574–576.

Vafai, K., Tien, C.L., 1981. Boundary and inertia effects on convective heat transfer in porous media. Int. J. Heat Mass Transfer 34, 195–203.

Wang, P., Kahawita, R., Nguyen, D.L., 1991. Transient laminar natural convection from horizontal cylinder. Int. J. Heat Mass Transfer 34, 1429–1442.